ECS Electrochemistry Letters, **2** (9) F64-F67 (2013)
2162-8726/2013/2(9)/F64/4/$31.00 © The Electrochemical Society

Analytical Description of a Dead Spot in a PEM Fuel Cell Anode

A. A. Kulikovsky[a,*,z] **and P. Berg**[b,*]

[a]*Institute of Energy and Climate Research, Electrochemical Process Engineering (IEK–3), Research Center Juelich, D-52425 Juelich, Germany*
[b]*Department of Physics, NTNU, 7491 Trondheim, Norway*

We report an analytical solution to a problem of the electric potential and local current distribution around a dead spot in a PEM fuel cell anode. The dead spot is modeled as a circular domain with zero exchange current density of the hydrogen oxidation reaction (HOR). Recent numerical studies (A. A. Kulikovsky. JES, **160** (2013) F401) revealed the formation of a current double layer at the spot boundary, with the peak of the HOR current just outside the spot. Here, we derive and discuss analytical expressions which elucidate the underlying problem.
 [DOI: 10.1149/2.004309eel]

Manuscript submitted April 23, 2013; revised manuscript received May 30, 2013. Published June 20, 2013.

Polymer electrolyte membrane fuel cells (PEMFCs) are close to commercialization, with automotive companies expected to begin mass production of PEMFC–powered cars in the next few years. Nonetheless, the lifetime of fuel cells still needs to be substantially improved to make this technology less expensive and more reliable.

Over the past decade, large efforts have been directed toward understanding the microscopic mechanisms of PEMFC degradation.[1] Some of these mechanisms include parasitic electrochemical reactions, which run many orders of magnitude faster in the domains where the reaction overpotential is larger. This raises the problem of local non–uniformities in fuel cells, which can produce large local overpotentials.

In this work, we continue the study of a problem of potentials and current distributions in the domain near a dead spot in the anode catalyst layer of a PEMFC. The spot of no or low electrochemical activity may arise due to local poisoning of the catalyst surface, or due to delamination of the anode catalyst from the membrane. Last but not least, this problem arises in the transmission X–ray absorption spectroscopy of the PEMFC cathode.[2,3] Transmission XAS requires removal of Pt atoms from a small circular anode "window" to make it transparent to X–rays probing the state of Pt atoms in the cathode catalyst layer (CCL).

In a previous analysis, the problem has been formulated and solved numerically.[4] The numerical solution reveals the formation of a current double layer (CDL) at the spot boundary. The main feature of this layer is a high HOR current density generated in a narrow ring just outside the spot ("hot ring"). Here, we report an analytical solution of the problem. This solution allows us to derive a simple relation for the characteristic width of the hot ring. The solution confirms the conjecture of[4] that the CDL is an autonomous structure, which is independent of the spot radius.

Model

Consider a domain with a circular dead spot; the system of coordinates is shown in Figure 1. The model is based on the following assumptions, which are discussed in more detail in the Results and Discussion section.

- The spot radius largely exceeds the membrane thickness. This allows us to reduce a 2D problem to a quasi–2D formulation.
- The ORR and HOR current densities obey Butler–Volmer kinetics.
- Transport losses in the cathode and anode catalyst layer are ignored.

Under these assumptions, the 2D Laplace equation for the membrane phase potential Φ

$$\frac{1}{r}\frac{\partial}{\partial r}\left(r\frac{\partial \Phi}{\partial r}\right)+\frac{\partial^2 \Phi}{\partial z^2}=0 \qquad [1]$$

reduces to a 1D Poisson equation[4]

$$\frac{1}{r}\frac{\partial}{\partial r}\left(r\frac{\partial \Phi}{\partial r}\right)=\frac{j^c-j^a}{\sigma_m l_m} \qquad [2]$$

where σ_m is the membrane proton conductivity, l_m the membrane thickness, and j^a, j^c are the HOR and ORR current densities coming in and out of the membrane, respectively.

To simplify calculations, we introduce dimensionless variables

$$\tilde{r}=\frac{r}{R_s},\quad \tilde{j}=\frac{j l_m}{\sigma_m b_{ox}},\quad \tilde{\Phi}=\frac{\Phi}{b_{ox}},\quad \tilde{b}_{hy}=\frac{b_{hy}}{b_{ox}} \qquad [3]$$

where R_s is the spot radius, b_{ox} and b_{hy} are the ORR and HOR Tafel slopes. Note that all the potentials are scaled to b_{ox}.

With these variables, Eq. 2 reduces to

$$\epsilon^2\frac{1}{\tilde{r}}\frac{\partial}{\partial \tilde{r}}\left(\tilde{r}\frac{\partial \tilde{\Phi}}{\partial \tilde{r}}\right)=\tilde{j}^c-\tilde{j}^a \qquad [4]$$

where

$$\epsilon=\frac{l_m}{R_s}. \qquad [5]$$

Assuming that the anode is grounded, dimensionless ORR and HOR current densities at the cathode and the anode, respectively, are given by[4]

$$\tilde{j}^c=2\tilde{j}^{\infty}_{ox}\sinh\left(\tilde{\Phi}+\tilde{E}^{eq}_{ORR}-\tilde{\phi}_c\right) \qquad [6]$$

$$\tilde{j}^a=2\tilde{j}^{\infty}_{hy}H(\tilde{r}-1)\sinh\left(-\frac{\tilde{\Phi}}{\tilde{b}_{hy}}\right) \qquad [7]$$

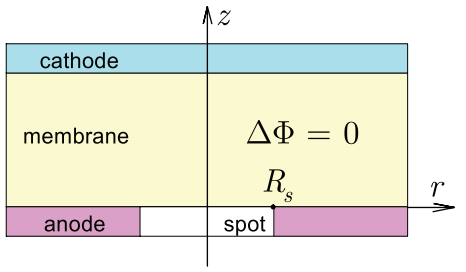

Figure 1. Schematic of the anode spot and the system of coordinates. Note that the figure is not to scale: in fact, the spot radius largely exceeds the membrane thickness. Note also that as the transport losses inside the catalyst layers are ignored, these layers can be treated as infinitely thin interfaces.

*Electrochemical Society Active Member.
[z]E-mail: kulikovsky@fz-juelich.de

where $\tilde{E}^{eq}_{ORR}$ is the equilibrium ORR potential, $\tilde{\phi}_c$ is the carbon phase potential on the cathode side (the cell potential), $\tilde{j}^{\infty}_{ox}$, $\tilde{j}^{\infty}_{hy}$ are the ORR and HOR exchange current densities, H is a Heaviside function which describes the step change of the HOR exchange current density from $\tilde{j}^{\infty}_{hy}$ at $\tilde{r} > 1$ to zero inside the spot, $\tilde{r} \le 1$.

With Eqs. 6, 7, the basic equation for $\tilde{\Phi}$, Eq. 4 takes the form

$$\epsilon^2 \frac{1}{\tilde{r}} \frac{\partial}{\partial \tilde{r}} \left(\tilde{r} \frac{\partial \tilde{\Phi}}{\partial \tilde{r}} \right) = 2\tilde{j}^{\infty}_{ox} \sinh\left(\tilde{\Phi} + \tilde{E}^{eq}_{ORR} - \tilde{\phi}_c\right) + 2\tilde{j}^{\infty}_{hy} H(\tilde{r} - 1) \sinh\left(\frac{\tilde{\Phi}}{\tilde{b}_{hy}}\right). \quad [8]$$

We have to consider Eq. 8 inside the spot area and outside the spot separately.

The Analytical Solution

Inside the spot area.— Inside the spot area ($0 \le \tilde{r} \le 1$), the HOR current is zero and Eq. 8 simplifies to

$$\epsilon^2 \frac{1}{\tilde{r}} \frac{\partial}{\partial \tilde{r}} \left(\tilde{r} \frac{\partial \tilde{\Phi}}{\partial \tilde{r}} \right) = 2\tilde{j}^{\infty}_{ox} \sinh\left(\tilde{\Phi} + \tilde{E}^{eq}_{ORR} - \tilde{\phi}_c\right). \quad [9]$$

We assume that the ORR overpotential is sufficiently large: $\tilde{\eta}_{ox} = \tilde{\Phi} + \tilde{E}^{eq}_{ORR} - \tilde{\phi}_c > 1$. At cell currents of practical interest this condition holds. Thus, in Eq. 9 we approximate the sinh–function by the dominating branch of the two corresponding exponential functions (Tafel approximation), and this equation reduces to

$$\epsilon^2 \frac{1}{\tilde{r}} \frac{\partial}{\partial \tilde{r}} \left(\tilde{r} \frac{\partial \tilde{\Phi}}{\partial \tilde{r}} \right) = \tilde{j}^{\infty}_{ox} \exp\left(\tilde{\Phi} + \tilde{E}^{eq}_{ORR} - \tilde{\phi}_c\right), \quad \left.\frac{\partial \tilde{\Phi}}{\partial \tilde{r}}\right|_{\tilde{r}=0} = 0, \quad \tilde{\Phi}(0) = \tilde{\Phi}_0. \quad [10]$$

Here, $\tilde{\Phi}_0$ is to be determined by matching conditions (see further below).

The problem Eq. 10 has been solved in Ref. 5 for $\tilde{\Phi}_0 = 0$. Straightforward extension of the result yields

$$\tilde{\Phi} = \tilde{\Phi}_0 - \ln\left(\left(1 - \frac{\tilde{j}_0}{8\epsilon^2}\tilde{r}^2\right)^2\right) \quad [11]$$

where $\tilde{j}_0$ is the ORR current density at the spot center:

$$\tilde{j}_0 = \tilde{j}^{\infty}_{ox} \exp\left(\tilde{\Phi}_0 + \tilde{E}^{eq}_{ORR} - \tilde{\phi}_c\right). \quad [12]$$

Note that $\tilde{j}_0$ exponentially depends on $\tilde{\Phi}_0$.

From Eq. 11, it follows that the characteristic length of the $\tilde{\Phi}$ variation inside the spot is

$$\Delta\tilde{r}_{ORR} \simeq \frac{\sqrt{8}\,\epsilon}{\sqrt{\tilde{j}_0}}. \quad [13]$$

Thus, inside the ring $1 - \Delta\tilde{r}_{ORR} \le \tilde{r} \le 1$, the variation of the ORR current density is not large. As $\tilde{j}_0 < \tilde{J}$, a lower estimate for $\Delta\tilde{r}_{ORR}$ is obtained if we replace $\tilde{j}_0$ by the mean current density $\tilde{J}$. Thus,

$$\Delta\tilde{r}_{ORR} \gtrsim \frac{\sqrt{8}\,\epsilon}{\sqrt{\tilde{J}}} \quad [14]$$

holds. This result is important for XAS measurements, as the state of Pt atoms inside the ring $1 - \Delta\tilde{r}_{ORR} \le \tilde{r} \le 1$ is close to their state in the undisturbed domain of the cell, and hence this ring can be used for XAS studies of the CCL (see Ref. 6 for more details).

Outside the spot area.— Outside the spot ($\tilde{r} > 1$), Eq. 8 takes the form

$$\epsilon^2 \frac{1}{\tilde{r}} \frac{\partial}{\partial \tilde{r}} \left(\tilde{r} \frac{\partial \tilde{\Phi}}{\partial \tilde{r}} \right) = 2\tilde{j}^{\infty}_{ox} \sinh\left(\tilde{\Phi} + \tilde{E}^{eq}_{ORR} - \tilde{\phi}_c\right) + 2\tilde{j}^{\infty}_{hy} \sinh\left(\frac{\tilde{\Phi}}{\tilde{b}_{hy}}\right), \quad [15]$$

$$\tilde{\Phi}(\infty) = \tilde{\Phi}^{\infty}.$$

At a large distance from the spot center $\partial\tilde{\Phi}/\partial\tilde{r} = 0$ and the equation for $\tilde{\Phi}^{\infty}$ is obtained by equating the right side of Eq. 15 to zero:

$$2\tilde{j}^{\infty}_{ox} \sinh\left(\tilde{\Phi}^{\infty} + \tilde{E}^{eq}_{ORR} - \tilde{\phi}_c\right) + 2\tilde{j}^{\infty}_{hy} \sinh\left(\frac{\tilde{\Phi}^{\infty}}{\tilde{b}_{hy}}\right) = 0. \quad [16]$$

Far from the spot area, $\tilde{\Phi} \simeq \tilde{\Phi}^{\infty}$. Near the spot boundary, a small variation in the HOR overpotential leads to a high HOR current. The small variation in $\tilde{\eta}_{hy}$ is caused by a small variation in $\tilde{\Phi}$, and hence we may write $\tilde{\Phi} = \tilde{\Phi}^{\infty} + \hat{\Phi}$, where $\hat{\Phi}$ is small. Substituting this into Eq. 15 and expanding the right side of this equation up to linear order in $\hat{\Phi}$, we find an equation

$$\epsilon^2 \frac{1}{\tilde{r}} \frac{\partial}{\partial \tilde{r}} \left(\tilde{r} \frac{\partial \hat{\Phi}}{\partial \tilde{r}} \right) = m^2 \hat{\Phi}, \quad \hat{\Phi}(\infty) = 0 \quad [17]$$

where

$$m = \sqrt{2\tilde{j}^{\infty}_{ox} \cosh\left(\tilde{\Phi}^{\infty} + \tilde{E}^{eq}_{ORR} - \tilde{\phi}_c\right) + \frac{2\tilde{j}^{\infty}_{hy}}{\tilde{b}_{hy}} \cosh\left(\frac{\tilde{\Phi}^{\infty}}{\tilde{b}_{hy}}\right)}. \quad [18]$$

The solution of equation 17 vanishing at infinity is the modified Bessel function of the second kind, $K_0(m\tilde{r}/\epsilon)$. With this, we obtain,

$$\tilde{\Phi} = \tilde{\Phi}^{\infty} + \gamma K_0(m\tilde{r}/\epsilon) \quad [19]$$

where γ is a constant determined by the matching condition (see below).

Matching conditions.— We now have to match the inner and outer solutions Eq. 11 and Eq. 19, respectively, at $\tilde{r} = 1$, to determine the constants $\tilde{\Phi}_0$ and γ. We know that $\tilde{\Phi}(\tilde{r})$ is continuous and smooth at $\tilde{r} = 1$ (while its second derivative is discontinuous). Hence, we require

$$\tilde{\Phi}_0 - \ln\left(\left(1 - \frac{\tilde{j}_0}{8\epsilon^2}\right)^2\right) = \tilde{\Phi}^{\infty} + \gamma K_0(m/\epsilon), \quad \text{(continuity)} \quad [20]$$

and

$$\frac{\tilde{j}_0}{2\epsilon^2} \frac{1}{\left(1 - \frac{\tilde{j}_0}{8\epsilon^2}\right)} = \frac{\gamma m}{\epsilon} K_0'(m/\epsilon), \quad \text{(smoothness)} \quad [21]$$

where the symbol "prime" means derivative over the argument.

Solving Eq. 21 for γ and substituting it into Eq. 20 yields a nonlinear equation for $\tilde{\Phi}_0$

$$\tilde{\Phi}_0 - \ln\left(\left(1 - \frac{\tilde{j}_0}{8\epsilon^2}\right)^2\right) = \tilde{\Phi}^{\infty} + \frac{\tilde{j}_0}{2\epsilon m} \frac{1}{\left(1 - \frac{\tilde{j}_0}{8\epsilon^2}\right)} \frac{K_0(m/\epsilon)}{K_0'(m/\epsilon)}. \quad [22]$$

Note that the parameter $\tilde{j}_0$ depends on $\tilde{\Phi}_0$ according to equation 12 and that the value of γ results from equation 21 once $\tilde{\Phi}_0$ has been computed. This finally determines our analytical solution uniquely.

The width of the HOR peak and the characteristic currents.— Due to the smallness of ϵ, the parameter m/ϵ appearing in the argument of the Bessel functions is large. This allows us to use the asymptotic expansions for K_0 and K_0'

$$K_0(\alpha\tilde{r}) \simeq -K_0'(\alpha\tilde{r}) \simeq \sqrt{\frac{\pi}{2}} \frac{\exp(-\alpha\tilde{r})}{\sqrt{\alpha\tilde{r}}}, \quad \alpha\tilde{r} \gg 1. \quad [23]$$

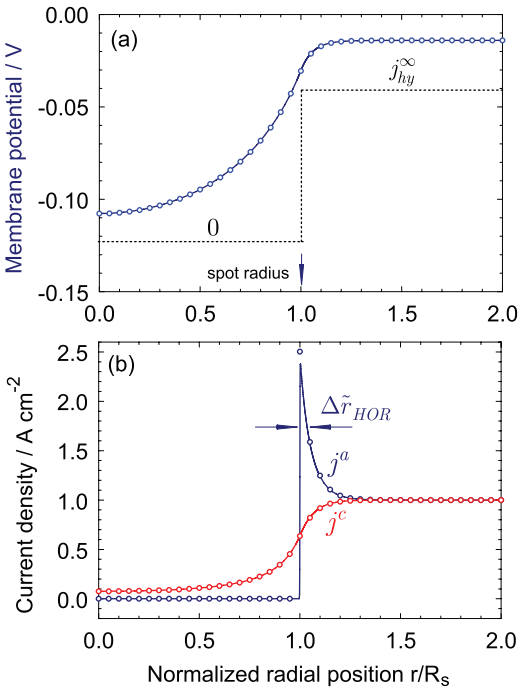

Figure 2. (a) The membrane potential and (b) the ORR and HOR current densities. Dots – the analytical solution, solid lines – the numerical result from the ODE solver. The dashed line in (a) indicates schematically the step shape of the HOR exchange current density. The spot radius corresponds to $r/R_S = 1$. $\Delta\tilde{r}_{HOR}$ depicts the FWHM of the HOR current density peak.

Eq. 23 enables us to estimate the width of the peak of the HOR current density $\Delta\tilde{r}_{HOR}$ just outside the spot (Figure 2). The $\tilde{r}$–dependence of $\tilde{\Phi}$ outside the spot is given by Eq. 19. From Eq. 23 we see, that the characteristic scale of the $\tilde{\Phi}$ variation is $1/\alpha$, where $\alpha = m/\epsilon$. The HOR current density $\tilde{j}_{hy}$ exponentially depends on $\tilde{\Phi}$, (see Eq. 7), and hence the scale of the $\tilde{j}_{hy}$ variation just outside the spot also is $\Delta\tilde{r}_{HOR} \simeq \epsilon/m$.

Further, from Eq. 18 it follows that $m \gtrsim \sqrt{(1+\tilde{b}_{hy}^{-1})\tilde{J}}$, where $\tilde{J}$ is the mean undisturbed current density. Indeed, the first term under the square root in Eq. 18 is on the order of the ORR current density in the undisturbed domain (which is $\tilde{J}$), while the second term is on the order of $\tilde{J}/\tilde{b}_{hy}$, where $\tilde{b}_{hy} \lesssim 1$ (Table I). Thus, the lower estimate for the sum under the square root in Eq. 18 is $\sqrt{2\tilde{J}}$, and we finally find

$$\Delta\tilde{r}_{HOR} \simeq \frac{\epsilon}{\sqrt{2\tilde{J}}}. \qquad [24]$$

Table I. The base–case physical parameters. Note that the spot radius is ten times the membrane thickness.

ORR exchange current density j_{ox}^{∞}, A cm^{-2}	10^{-6}
ORR equilibrium potential E_{ox}^{eq}, V	1.23
ORR Tafel slope b_{ox}, V	0.0364
HOR exchange current density in the regular domain j_{hy}^{∞}, A cm^{-2}	1
HOR Tafel slope b_{hy}, V	0.0291
Membrane proton conductivity σ_m, Ω^{-1} cm^{-1}	0.1
Membrane thickness l_m, cm	0.0025 (25 μm)
Spot radius R_s, cm	$10l_m = 0.025$
Cell potential ϕ_c, V	0.7131
Mean current density in the regular domain J, A cm^{-2}	1.0
Cell temperature T, K	273 + 65

In dimensional form, Eq. 24 reads

$$\Delta r_{HOR} \simeq \sqrt{\frac{\sigma_m b_{ox} l_m}{2J}} \qquad [25]$$

and hence Δr_{HOR} is independent of the spot radius R_s. Thus, the structure of the current double layer at the spot boundary is independent of the spot radius, as it has been assumed in Ref. 4.

Eq. 11 allows us to calculate the mean ORR current density in front of the spot,

$$\tilde{J}_s = \frac{1}{\pi}\int_0^1 \tilde{j}^c(\tilde{r})2\pi\tilde{r}\,d\tilde{r}.$$

The local ORR current inside the spot, j^c, is given by Eq. 6. With $\tilde{\Phi}$ from Eq. 11, we obtain[†]

$$\tilde{J}_s = \frac{\tilde{j}_0}{1-\dfrac{\tilde{j}_0}{8\epsilon^2}}. \qquad [27]$$

Another parameter of interest is the peak HOR current density. The HOR current density is given by $\tilde{j}^a = 2\tilde{j}_{hy}^{\infty}\sinh(-\tilde{\Phi}/\tilde{b}_{hy})$. Clearly, the peak current is reached at $\tilde{r} = 1$: $\tilde{j}_1^a = \tilde{j}^a(1)$. Using, e.g., the left side of Eq. 20 for $\tilde{\Phi}(1)$, for the peak current density we find the following equation

$$\tilde{j}_1^a = -2\tilde{j}_{hy}^{\infty}\sinh\left(\frac{\tilde{\Phi}^{\infty}+\gamma K_0(m\tilde{r}/\epsilon)}{\tilde{b}_{hy}}\right). \qquad [28]$$

where $\tilde{\Phi}^{\infty}$ is the solution to Eq. 16.

Results and Discussion

Calculations with the equations above include the numerical solution of the nonlinear equation 22 for the membrane potential at the spot center $\tilde{\Phi}_0$. Once $\tilde{\Phi}_0$ is calculated, the parameter γ follows from Eq. 21. With $\tilde{\Phi}_0$ and γ, the shapes of $\tilde{\Phi}$ inside and outside the spot are determined by Eqs.11 and 19, respectively.

Figure 2 shows a comparison of a direct numerical solution of the differential equation 8 (solid lines) and analytical (dots) radial shapes of the membrane potential Φ and ORR and HOR current densities. Parameters for the calculation are listed in Table I (the parameters are the same as in Ref. 4). As can be seen, the analytical solution is in excellent agreement with the numerical curves from the ODE solver.

Figure 2 shows also the numerical full width at half–maximum (FWHM) of the peak of the HOR current. This value in Figure 2 is 0.04, while Eq. 25 gives a number twice as large, 0.085. The discrepancy is due to the underestimated parameter m, as discussed in Section 3.4. Nonetheless, Eq. 25 gives a reasonable upper estimate for $\Delta\tilde{r}_{HOR}$.

Of large interest is the peak value of the HOR current density, j_1^a. Unfortunately, due to the strong nonlinearity of Eq. 22, we were not able to obtain a simple explicit approximation for this value. Numerical calculations with Eq. 28 are shown in Figure 3. In the region of large cell currents, the peak HOR current density j_1^a depends almost linearly on the mean cell current density J (Figure 3). Note that the slope of the curves in Figure 3 increases with a decrease in ϵ, which is equivalent to an increase in the spot radius. In other words, in larger spots the peak HOR current grows faster with the cell current. Note also that the variation of the peak current with ϵ is small: quadrupling ϵ changes j_1^a by $\simeq 10\%$ only. This result also shows that

[†]From Eq. 27 we see that

$$1-\frac{\tilde{j}_0}{8\epsilon^2} = \frac{\tilde{j}_0}{\tilde{J}_s}. \qquad [26]$$

As $\tilde{j}_0 < \tilde{J}_s$, the following relation holds

$$0 < 1-\frac{\tilde{j}_0}{8\epsilon^2} \le 1.$$

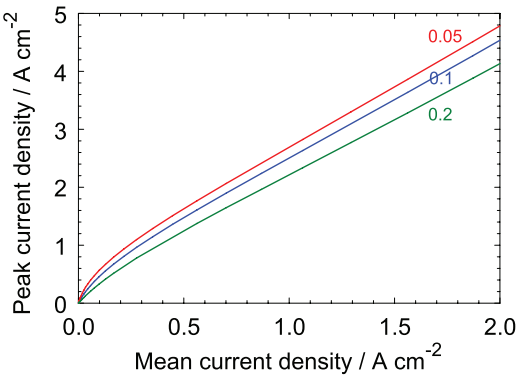

Figure 3. The peak HOR current density versus the mean cell current density J for the indicated values of ϵ. Parameters are listed in Table I.

the structure of the current double layer is independent of ϵ, provided that $\epsilon \ll 1$.

Physically, the current double layer forms to balance proton currents in the system. As the anode spot does not produce protons, the ORR overpotential in front of the spot tends to decrease in order to lower the ORR current density there. Lowering of the ORR overpotential requires lowering of Φ in the spot area, which, in turn, means formation of a radial gradient of Φ (Figure 2). The peak of the HOR current density forms to provide the radial proton current corresponding to the radial gradient of Φ inside the membrane.

Physically, the discontinuity of the HOR exchange current at $\tilde{r} = 1$ is justified if the width of the transition region between the spot area and the undisturbed domain is much smaller, than the spot radius. For large spots ($R_s \gg l_m$), this assumption seems quite reasonable. In this case, the peak current is independent of the actual shape of the exchange current density inside the transition region. This has been verified with the numerical model.

Our primary goal is to understand the main effect and to rationalize the parametric dependencies in the problem. For this reason, we have employed a simplified model of catalyst layers performance, which ignores all transport losses in the cell. Note that the main effect (peak HOR current) arises on the anode side, where the transport of hydrogen is fast. On the cathode side, the ORR current density inside the spot is much lower, than in the undisturbed domain. Thus we may expect that incorporation of the hydrogen and oxygen transport into the model would have a minor effect on the results.

An uncertainty in our model is the quasi–2D description of the rapidly changing HOR current at the spot interface. A full 2D solution is necessary to understand the quality of the quasi–2D shapes at this interface. Nonetheless, the gradient of Φ at $\tilde{r} = 1$ is not large (Figure 2), and we expect that the quasi–2D model is reasonably accurate.

It is worth mentioning that if the hydrogen feed stream is not humidified, a large HOR current at the spot boundary may dry out the membrane. This could be another detrimental effect of the dead spot. In that case, the model can be used to estimate the rate of membrane drying.

Lastly, it should be pointed out that while full 2D numerical simulations are required to analyze the system in detail and relax some of the constraints, the assumptions in this paper allow for an analytical solution that helps formulate estimates for the characteristic values.

Conclusions

We reported an analytical solution to a problem of the local current distribution around a dead spot in an anode catalyst layer. Such a spot can arise due to local catalyst poisoning, or it can be made deliberately to provide a Pt–free window for X–ray spectroscopy studies of the cell cathode. We derived analytical expressions for the distribution of membrane potential and for local current densities at the electrodes in and around the spot. The solution confirms the formation of the current double layer (CDL) at the spot boundary and it gives parametric dependencies for the CDL characteristic widths inside and outside the spot. The results can be used for accurate XAS measurements of PEMFC cathodes and for aging studies.

Acknowledgments

P. Berg thank I. Simonsen for the discussions about Bessel functions.

List of Symbols

$\Delta\tilde{r}_{ORR}$	Characteristic scale of the ORR current density variation, cm
ϵ	Dimensionless parameter, Eq. 5
γ	Dimensionless parameter, Eq. 19
Φ	Membrane potential, V
Φ^{∞}	Membrane potential at $r = \infty$, V
Φ_0	Membrane potential at $r = 0$, V
ϕ_a	Carbon phase potential of the anode, V
ϕ_c	Carbon phase potential of the cathode, V
σ_m	Membrane proton conductivity, Ω^{-1} cm^{-1}
b_{hy}	HOR Tafel slope, V
b_{ox}	ORR Tafel slope, V
E^{eq}	Equilibrium half–cell potential, V
H	Heaviside function
J	Mean cell current density in the undisturbed domain, A cm^{-2}
j^a	HOR current density, A cm^{-2}
j^c	ORR current density, A cm^{-2}
j_0	ORR current density at $r = 0$, A cm^{-2}
J_s	Mean ORR current density inside the spot, A cm^{-2}
j_{hy}^{∞}	HOR undisturbed exchange current density, A cm^{-2}
j_{ox}^{∞}	ORR exchange current density, A cm^{-2}
K_0	Modified Bessel function of the second kind
l_m	Membrane thickness, cm
m	Dimensionless parameter, Eq. 18
r	Radial position, cm
R_s	Spot radius, cm
z	Axial position, cm

References

1. R. Borup et al., *Chem. Rev.*, **107**, 3904 (2007).
2. A. E. Russell and A. Rose, *Chem. Rev.*, **104**, 4613 (2004).
3. C. Roth, N. Benker, M. Mazurek, and F. S. H. Fuess, *Adv. Eng. Mater.*, **7**, 952 (2005).
4. A. A. Kulikovsky, *J. Electrochem. Soc.*, **160**, F401 (2013).
5. P. Berg and K. Ladipo, *Proc. Roy. Soc. A*, **465**, 2663 (2009).
6. A. A. Kulikovsky, *J. Solid State Electrochem.* (under review) (2013).